

CHROM. 15,240

DESIGN OF A POST-COLUMN FLUORESCENCE DERIVATIZATION SYSTEM FOR USE WITH MICROBORE COLUMNS

P. KUCERA* and H. UMAGAT

Pharmaceutical Research Products Section, Quality Control Department, Hoffmann-La Roche Inc., Nutley, NJ 07110 (U.S.A.)

SUMMARY

The design of a post-column fluorescence derivatization system utilizing microbore columns is discussed theoretically and investigated experimentally. The basic disadvantage with post-column derivatization systems is the introduction of additional band broadening that occurs in the flow-through reactor. In this paper, the band spreading in the reactor is limited by using a zig-zag open-tubular capillary, where plate height decreases with the square of the capillary diameter. It is shown that adequate mixing of two liquid streams can be achieved with a special 30-nl volume mixing chamber. Some of the reactor design parameters are, by necessity, based on the model fluorescence derivatization reaction employed; in this case, a modification of the very fast *o*-phthalaldehyde reaction with primary amines is reported which incorporates the use of 3-mercaptopropionic acid. The consideration of the minimum allowable residence time and the minimum band spreading in the reactor and the mixing chamber allows calculation of the reactor geometry. Theoretical investigation of the reactor design allows prediction of the general rules for the system optimization. The application of the system to analysis of amino acids and primary aliphatic amines, which were separated on an octadecyl-silica reversed-phase column, is demonstrated. Advantages and disadvantages of the system are discussed.

INTRODUCTION

The use of microbore columns in liquid chromatography has been demonstrated recently¹⁻⁴ and various advantages associated with the reduction of the diameter of an analytical column have been reported^{5,6}. However, on-line fluorescence derivatization techniques employed in conjunction with narrow-bore packed columns, which could achieve high specificity and better sensitivity of detection, have not been investigated in great detail. One reason for this was probably the lack of sufficiently sensitive low cell volume fluorescence detectors which could be used with microbore columns. Other reasons were related to the complexity of microbore instrumentation or misunderstanding of the parameters necessary for the total system optimization.

Of the two possible methods of chemical derivatization, namely, the pre-column and the post-column derivatization, the latter is considered to be more inter-

esting from the theoretical as well as experimental points of view. Although both of these techniques are usually carried out to enhance solute detectability and specificity of detection and may have particular advantages in a given situation, the major advantage of the post-column system results from the fact that chromatographic conditions necessary to achieve the desired resolution do not have to be changed, as is the case when the precolumn technique is employed. However, derivatization of components after chromatography as they emerge from the column necessitates the introduction of some form of continuous reactor which inevitably leads to dispersion of chromatographic bands. Quite clearly, the band spreading resulting from the solute residence in the reactor must be kept to a minimum to prevent closely eluting substances from remixing. Other prerequisites of the post-column system require that the reagent employed must not exhibit a high background detector signal and there must be total compatibility of the mobile phase and the reagent medium. As demonstrated earlier, the flow-rate of the mobile phase through the column, the maximum solute volume and mass placed on the column, the detector cell and peak volumes, and also the volume of the flow-through reactor used with 4.6-mm I.D. columns have to be scaled down proportionally with the square of the ratio of the respective column diameters, $(1/4.6)^2$, when using 1-mm I.D. microbore columns, assuming the same chromatographic conditions and solute residence time¹. While reactor residence times of several minutes have been tolerated in long chromatographic runs on large-diameter analytical columns operated at fast flow-rates, such conditions are unacceptable when using microbore columns of small diameters operated at slower flow-rates. Thus, the reaction times employed should be kept as short as possible⁷.

The major aim of this work was to design a practical post-column derivatization system which could be used with 1-mm I.D. microbore columns and to study the parameters necessary for system optimization. In order to achieve this goal, it was necessary to design a low-volume mixing chamber, to investigate radial mixing of two liquid streams under the conditions of an extremely small volume (30 n μ l), and to examine band spreading in various parts of the post-column system. Furthermore, experiments to determine the solute residence time and stability of the formed fluorescence adducts had to be carried out.

THEORY

Optimization of the post-column reaction system

The design of a post-column derivatization system is dependent primarily on the kinetics of the reaction employed in the derivatization, from which the minimum solute residence time, t_r , necessary for the solute to spend in the reaction coil is determined. For the purpose of this paper, t_r is considered nonvariant since it depends only upon the chemical reaction employed. It should be noted that, as the flow of the mobile phase through the column, Q_1 , necessary to achieve the desired resolution, and the reagent flow, Q_2 , are selected, the volume of the open-tubular reactor is fixed according to the following equation:

$$V_r = (Q_1 + Q_2) \cdot t_r = Q_1 \cdot t_r \cdot \psi = \frac{\pi D_r^2 \cdot L_r}{4} \quad (1)$$

where ψ is the dimensionless flow-rate parameter corresponding to the ratio of the total flow-to-column flow.

While keeping the reactor volume constant, the diameter (D_r) and length (L_r) can be independently varied. Assuming that two closely eluting peaks, A and B, are Gaussian in shape and have similar band widths ($\sigma_A = \sigma_B = \sigma_c$), then the maximum resolution that can be achieved on the given column can be expressed as

$$R_{\max} = \frac{(V_B - V_A)}{4\sigma}$$

where V_B and V_A are the elution volumes for solute B and A, respectively. Huber *et al.*⁸ pointed out recently that the introduction of the ideal mixing chamber with a secondary flow ($\psi > 1$) increases both the solute band width as well as the solute retention volume in direct proportion to the flow-rate parameter, ψ , whereas the maximum solute concentration varies inversely with ψ . Thus, in the case of ideal mixing, solute resolution should not be affected. In reality, the mixing chamber employed may contribute to band spreading. Using the principle of summation of variances and assuming that the solute band width increases by $p\%$ of σ_c as the solute passes through the mixing chamber, the total volume variance (σ_t^2) is given by

$$\sigma_t^2 = \sigma_c^2 + \sigma_m^2 = \sigma_c^2(1 + p)^2$$

and the resolution after the mixing chamber can be described by the following equation:

$$R_m = \frac{R_{\max}}{\sqrt{\left(1 + \frac{\sigma_m^2}{\sigma_c^2}\right)}} = \frac{R_{\max}}{(1 + p)} \quad (2)$$

where σ_m^2 is the volume variance arising from the mixing chamber and σ_c^2 is the column variance. As we interpose the reaction coil between the detector and the mixing chamber, the total variance, as measured by the detector, of negligible cell volume has to reflect the band dispersion due to the reactor, σ_r^2 .

$$R_r = \frac{R_{\max}}{\sqrt{\left(1 + \frac{\sigma_m^2}{\sigma_c^2} + \frac{\sigma_r^2}{\sigma_c^2} \psi^2\right)}} \quad (3)$$

Plate theory derives σ^2 as a ratio of V^2/N , where N is the number of theoretical plates in a given system and V is either solute retention volume for a packed column ($V_c = Q_1 \cdot t_c$) or reactor volume in the case of an open-tubular reactor. Thus, using the plate theory, eqn. 3 leads to the following expressions:

$$\begin{aligned} R_r &= \frac{R_{\max}}{\sqrt{\left(1 + p\right)^2 + \left(\frac{D_r}{D_c}\right)^4 \cdot \left(\frac{L_r}{L_c}\right)^2 \cdot \left(\frac{N_c}{N_r}\right) \cdot \frac{1}{(1 + k')^2 \cdot \psi^2 \cdot \epsilon^2}}} \\ &= \frac{R_{\max}}{\sqrt{\left(1 + p\right)^2 + \left(\frac{t_r}{t_0}\right)^2 \cdot \frac{N_c}{N_r(1 + k')^2}}} \end{aligned} \quad (4)$$

Subscripts r and c denote reactor and column conditions, respectively; k' is the solute capacity factor and ε is the total column porosity. According to eqn. 4, the ideal reactor may be defined as one where $R_r \rightarrow R_{\max}$. This can be achieved in the case of ideal mixing ($p = 0$) and under the conditions where the denominator in eqn. 4 approaches a value of 1. It can be seen from eqn. 4 that a much smaller reactor diameter and length, as compared to column parameters, and a large number of theoretical plates in the reactor (N_r) are desired in order to approach an "ideal" post-column reaction system. It has been shown⁹⁻¹¹ that, if $t_r > D_r^2/(4 \cdot D_m)$, the reactor volume variance can be expressed as follows:

$$(\sigma_r^2)_v = \frac{\pi \cdot D_r^4 \cdot L_r \cdot (Q_1 + Q_2)}{384 \cdot D_m} = \frac{V_r \cdot D_r^2 \cdot (Q_1 + Q_2)}{96 \cdot D_m} \quad (5)$$

and the reactor time variance is given as

$$(\sigma_r^2)_t = \frac{t_r \cdot D_r^2}{96 \cdot D_m}$$

where D_m is the diffusivity of the solute in the combined mobile phase-reagent medium operated at the linear velocity, u_r . Substituting the value $(\sigma_r^2)_v$ or $(\sigma_r^2)_t$ in eqn. 3, expressions for relative resolution as a function of column parameters and solute diffusivity are obtained:

$$\begin{aligned} \frac{R_r}{R_{\max}} &= \left[(1 + p)^2 + \left(\frac{D_r}{D_c} \right)^2 \frac{u_c \cdot N_c \cdot V_r}{(1 + k')^2 \cdot 24 \cdot D_m \cdot L_c^2 \cdot \pi \cdot \psi \cdot \varepsilon} \right]^{-1/2} \\ &= \left[(1 + p)^2 + \frac{D_r^2 \cdot t_r \cdot N_c}{96 \cdot D_m \cdot t_0^2 \cdot (1 + k')^2} \right]^{-1/2} \end{aligned} \quad (7)$$

It can be seen that reactor diameter, volume, and t_r have to be minimized in order to approach the "ideal" post-column reaction system. However, decreasing the reactor diameter at a given flow-rate increases the linear velocity and pressure in the reactor by a factor equal to the square of the ratio of respective reactor diameters. This phenomenon has a reducing effect on the number of theoretical plates that can be achieved in a given reactor. Nevertheless, reducing the reactor diameter at constant V_r results in introducing a longer reactor; this will inevitably increase the number of theoretical plates (N_r) which are desired. Obviously, the reactor diameter cannot be decreased indefinitely and is constrained by the maximum pressure rating of the instrumentation available. Considering a 450-bar pressure rating and a very fast reaction, such as that employed in this report ($t_r \approx 10$ sec), the use of 25- to 50- μm capillary reactors with microbore columns, 1 mm I.D., appears to be experimentally feasible.

EXPERIMENTAL

Solvents and reagents

Methanol, acetonitrile, tetrahydrofuran, and high-purity water were obtained from Burdick and Jackson (Muskegon, MI, U.S.A.). Amino acid standards, *o*-phthaldialdehyde (OPA), 2-mercaptoethanol, ethanethiol, and 3-mercaptopropionic acid were purchased from Pierce (Rockford, IL, U.S.A.). Sodium acetate and boric acid were analytical-grade reagents from Mallinckrodt (St. Louis, MO, U.S.A.). Samples of sulfonamides were obtained from Hoffmann-La Roche (Nutley, NJ, U.S.A.) and *n*-alkylamines were obtained from Aldrich (Milwaukee, WI, U.S.A.).

Chromatographic equipment

The system used consisted of two Waters Assoc. Model 6000A solvent delivery systems remote-controlled by Hewlett-Packard Model HP3311A function generators; and Kratos SF 970 fluorescence and SF 770 variable-wavelength UV detectors equipped with standard detector cells and specially designed micro cells of 0.25- and 0.5- μ l volume for the fluorescence and the UV detector, respectively. The UV detector was operated at 254 nm and the fluorescence detector was set at a 330-nm excitation wavelength using a 418-nm cut-off filter. Stainless-steel capillary tubing, fused-silica open-tubular columns of various diameters, and ODS microbore columns packed with Zorbax C₁₈ reversed-phase 7- μ m particles were obtained from Alltech (Deerfield, IL, U.S.A.). Microbore columns packed by the authors with similar materials were also employed. The detector was connected to a Hewlett-Packard Model HP1000 computer system with data collection and handling software provided by Computer Inquiry Systems (Allendale, NJ, U.S.A.). The sample was introduced with a Valco electrically actuated sampling valve equipped with a 0.2- μ l internal loop.

Chemical derivatization

To 1 g of OPA dissolved in 15 ml of methanol, 1 ml of the selected mercaptan was added and diluted to 200 ml with 0.4 M borate buffer (pH adjusted to 9.4 with 4M NaOH).

Effect of the nature of mercapto reagent on OPA reaction

The derivatization procedure using OPA is routinely performed in the analysis of primary amines and specifies the use of either mercaptoethanol or ethanethiol to form the highly fluorescent 1-alkylthio-2-alkyl substituted isoindoles¹²⁻¹⁴. The effect of various mercaptans on the reaction time, fluorescence response, and stability of the formed fluorescence OPA adducts was investigated. The reaction fluorescence-time profile and the stability of the formed adducts were monitored for each modification in the OPA reagent preparation in which various mercapto reagents were employed. As shown in Fig. 1, a continuous-flow closed system was used, with all the connecting tubing from the solvent delivery system to the detector and the detector back to the solvent reservoir minimized.

The pump was operated at its maximum capacity of 10 ml/min, and, initially, the system was equilibrated with the reagent, which consisted of OPA, and the mercaptan being studied solubilized in 0.4 M borate buffer pH = 9.4. Data acquisition was initiated at the time the test solute was added at the acquisition rate of 15 points

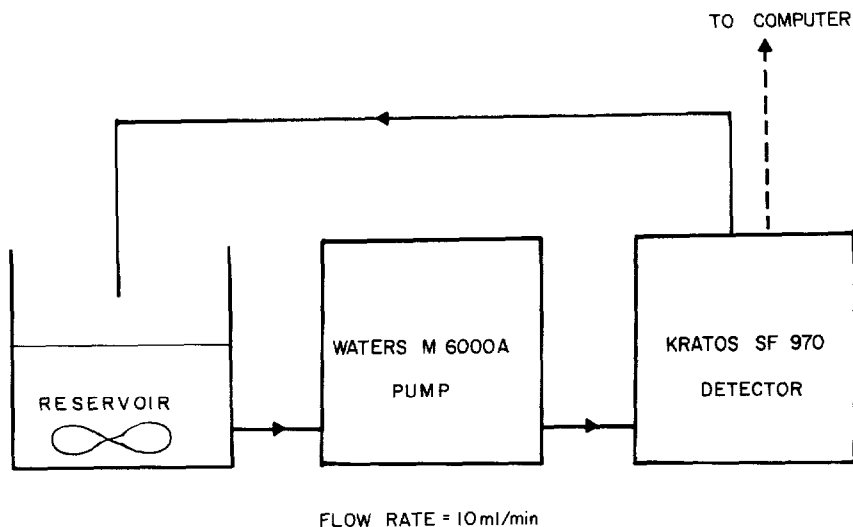


Fig. 1. Schematic diagram of a reaction system for the study of fast reactions.

per sec. To ensure instantaneous mixing, a minute volume of alanine solution, which was the test solute used, was employed in relation to the reagent volume. The solution was vigorously mixed during the entire period the fluorescence-time curve was determined. Within 10 sec, the OPA-alanine fluorescence adduct was formed and the reaction was then monitored for up to two hours to determine the rate of adduct degradation. A conventional fluorescence detector cell of $5\text{-}\mu\text{l}$ volume was employed in these experiments.

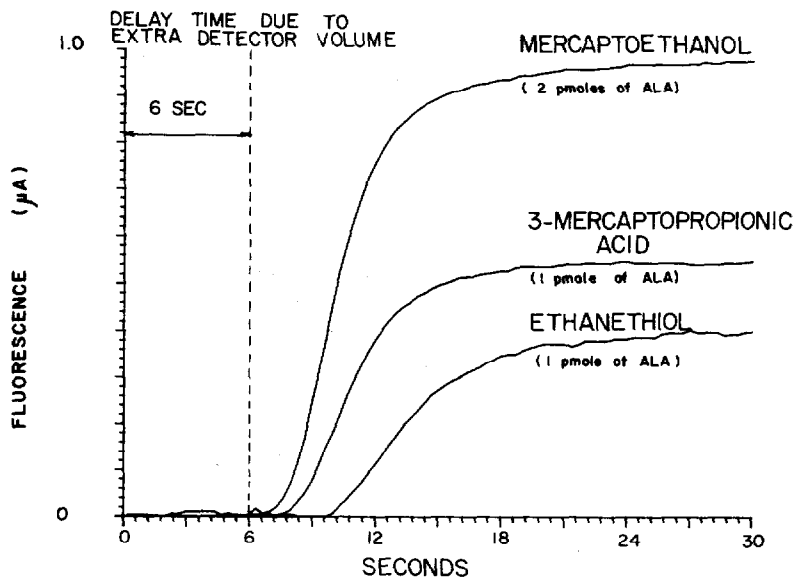


Fig. 2. Graphs relating fluorescence response to reaction time for OPA-alanine using various mercapto reagents.

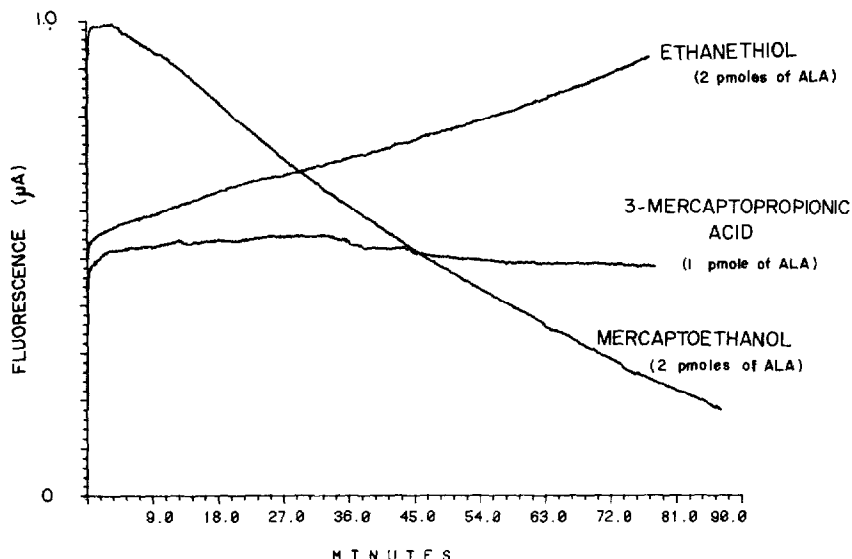
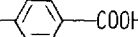
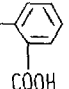


Fig. 3. Graphs demonstrating the effect of various mercapto reagents on the stability of OPA-alanine.

The results obtained are shown in Fig. 2 as graphs relating the fluorescence of OPA-alanine adducts to reaction time for three different mercapto reagents. The detector delay time resulting from extra detector dead volume was determined to be 6 sec at the given flow-rate. It can be seen that, for each of the mercapto reagents employed, about 9 sec reaction time was necessary to reach the maximum fluorescence intensity. Furthermore, the best fluorescence response for 1 pmole of alanine was obtained using OPA-3-mercaptopropionic acid reagent. Investigation of the stability of the formed fluorescence adducts (Fig. 3) revealed that a severe degradation of OPA-alanine occurred when employing mercaptoethanol as a reagent and an increase in the fluorescence intensity with time was observed with ethaneethiol reagent. Table I

TABLE I
EFFECT OF MERCAPTANS ON THE RESPONSE AND STABILITY OF OPA-ALANINE FLUORESCENT ADDUCT

Structure	Response	Stability
SH-CH ₂ -CH ₃	Low	Good (Fluorescence tends to increase with time)
SH-CH ₂ CH ₂ OH	Good	Poor
SH-CH ₂ COOH	Poor	Excellent
SH-CH ₂ CH ₂ COOH	Excellent	Excellent
SH-CH(CH ₃)-COOH	0	-
SH-CH(COOH)-CH ₂ COOH	Poor	Good
SH- 	Poor	Good
SH- 	Poor	Good

summarizes the results obtained from these experiments and shows a significant finding that OPA-3-mercaptopropionic acid adducts exhibit better stability and fluorescence response than other mercapto adducts investigated. This may be due to the stabilizing effect of the carboxylic group which also affects the fluorescence intensity of the isoindole ring.

Investigation of radial mixing using low-volume mixing chamber

Throughout this work, post-column derivatization experiments were carried out using the instrumental arrangement shown in Fig. 4. However, to study the efficiency of radial mixing of two liquid streams, the reactor was disconnected and a specially designed mixing chamber was connected directly to the UV detector (0.5- μ l cell volume). A special Valco mixing tee was laser drilled to 150 μ m I.D., and two 1/16 in. O.D. inlet/outlet ports for the column and the exit tubing were positioned at a 90° angle¹⁵. The distance separating the reagent tubing and the exit tubing was 1.8 mm, giving a total volume of the mixing chamber of about 30 nl. The extent of mixing of benzene with methanol was examined by mixing 0.1% (v/v) benzene in methanol and neat methanol at identical flow-rates, $Q_1 = Q_2 = 35 \mu$ l/min. Two Waters M6000A solvent delivery systems controlled by Hewlett-Packard frequency generators were used. The absorbance of the combined streams at 254 nm was recorded for each variation in the flow pattern design and modification of the mixing chamber, which can be seen in Fig. 5. The modifications of the mixing chamber were as follows: (D)

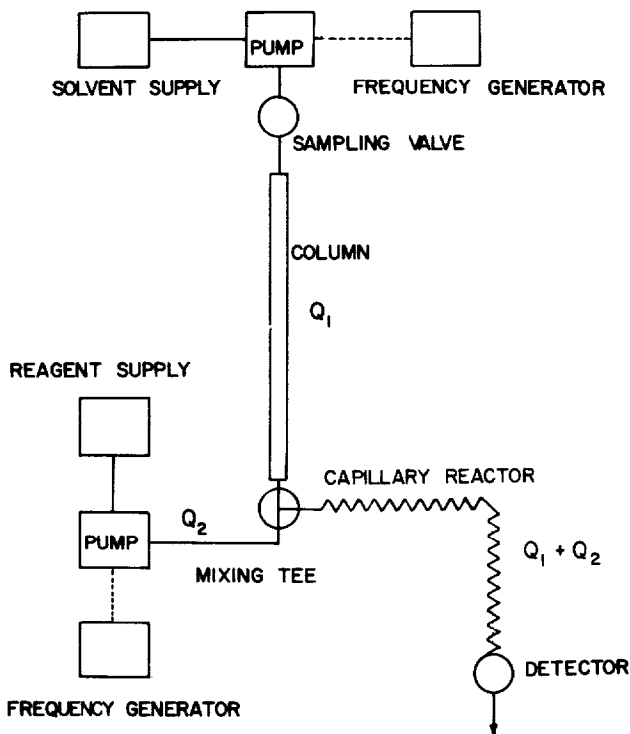


Fig. 4. Block diagram of a microbore post-column derivatization system.

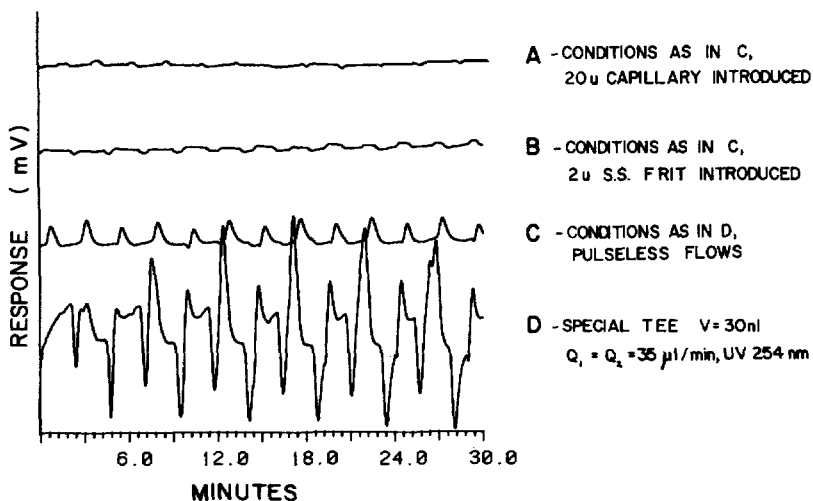


Fig. 5. Mixing patterns of benzene and methanol with different mixing designs.

mixing using special Valco mixing chamber only; (C) same as D plus modifications in the solvent delivery systems where built-in pulse dampers were installed; (B) conditions same as in C except that the mixing chamber was modified by introducing one 2- μ m stainless-steel frit on each of the three outlet ports; and (A) conditions same as in C and a fused-silica capillary (20 μ m I.D.) was inserted in the internal volume of the mixing tee. It can be seen in Fig. 5 that inadequate mixing was obtained when using the unmodified tee. The mixing disturbances could be traced to movements of the pistons in the pump heads, and installing the pump pulse dampers improved the mixing efficiency significantly. Further improvements were achieved by introducing flow obstacles into the stream path of the mixed medium, which probably generated eddies and improved the mixing efficiency.

Band dispersion arising from various parts of the post-column derivatization system

As the solute band passes through the column, mixing chamber, reactor, and to the detector, the band width increases. It is of interest to evaluate the band spread contribution from various components present in the post-column reaction system. The variances are additive, assuming that the contributing phenomena for variance are not interdependent; thus, the total variance in the detector of negligible volume should reflect the variance of the band leaving the column, the variance contribution due to dispersion in the mixing chamber, and the variance contributed by the capillary reactor¹⁶. As pointed out recently¹⁷, second statistical moments should be used when calculating variances arising from the asymmetric peaks frequently obtained by HPLC; thus, throughout this work, only second statistical moments were employed. The calculation of variance from statistical moments is shown in the Appendix. To evaluate the dispersion in the derivatization system, the peak widths of eight sulfonamides were determined, as they eluted from the microbore column. With this peak width as a reference, the additional band dispersion resulting from the mixing chamber, which is unavoidable when two liquid streams are being mixed, was measured. For this study, there was no reaction employed and the only flow involved

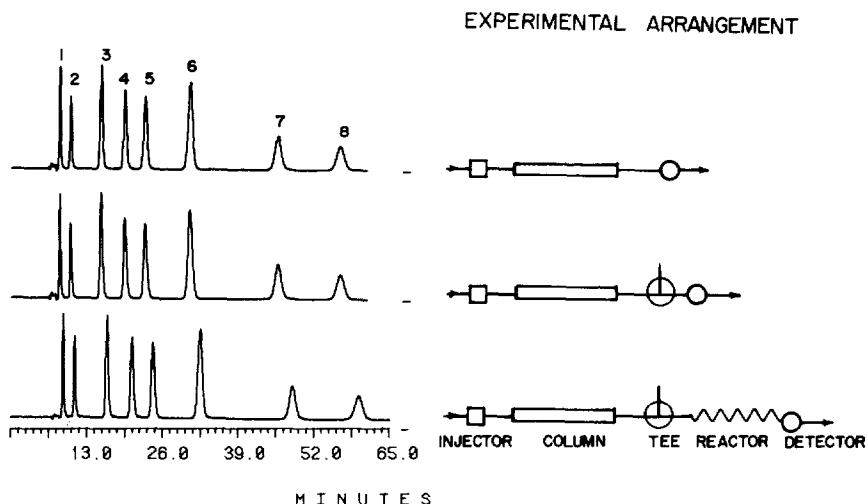


Fig. 6. Chromatograms demonstrating the band dispersion arising from various parts of the microbore post-column derivatization system. Solutes: 1 = sulfanilamide; 2 = sulfadiazine; 3 = sulfanilylsulfanilamide; 4 = isosulfamethoxazole; 5 = sulfisoxazole; 6 = sulfadimethoxine; 7 = acetylsulfamethoxazole; 8 = acetylsulfisoxazole. Concentration: 0.2 mg/ml for each test solute.

was from the chromatographic column, which was kept constant at 35 $\mu\text{l}/\text{min}$ ($\psi = 1$). The test mixture of sulfonamides was chromatographed on an Alltech ODS microbore column, 50 cm \times 1 mm I.D., using a mixture of 70% (v/v) 0.01 M KH_2PO_4 buffer, pH 3, and 30% (v/v) acetonitrile as the mobile phase. Chromatograms obtained from the test mixture using different experimental arrangements can be seen in Fig. 6. A stainless-steel reactor (176 cm \times 0.18 mm I.D.) with a volume of 44 μl was employed. Total mass placed onto the column was 50 ng and the detection was by UV absorbance at 254 nm. No increase in peak width after the solutes passed through the low-volume mixing chamber could be observed, which indicates nearly ideal mixing ($p = 0$). However, the 44- μl volume reactor caused an increase in band width of sulfadimethoxine ($k' = 4.8$) and acetylsulfisoxazole ($k' = 9.6$) of 2.5 and 2.2%, respectively. The results of the peak width measurements at 0.6063 of the height of the elution curve can be seen in Fig. 7. Despite the relatively large volume of the capillary reactor, only a 2% increase in the band width was observed, which is tolerable.

Effect of reactor diameter, volume and ψ on the total volume variance

A mixture of *n*-alkylamines was used to evaluate the band spreading resulting from the use of various reactors of different volume and diameter. The test mixture was chromatographed on an Alltech ODS 50 cm \times 1 mm I.D. column and derivatized on-line in the post-column mode with OPA-3-mercaptopropionic acid reagent. The diagram of the instrumental arrangement used is shown in Fig. 4.

Using a constant reactor volume of 40 μl and a combined flow of 70 $\mu\text{l}/\text{min}$ ($Q_1 = Q_2 = 35 \mu\text{l}/\text{min}$), chromatograms of the test mixture were obtained for each variation in the diameter of the reactor used. Throughout these experiments, stainless-steel tubing of 0.007, 0.009, 0.02, and 0.03 in. I.D. were employed as reactors. The tubing was zig-zagged to 180 waves per meter to introduce a secondary flow phenom-

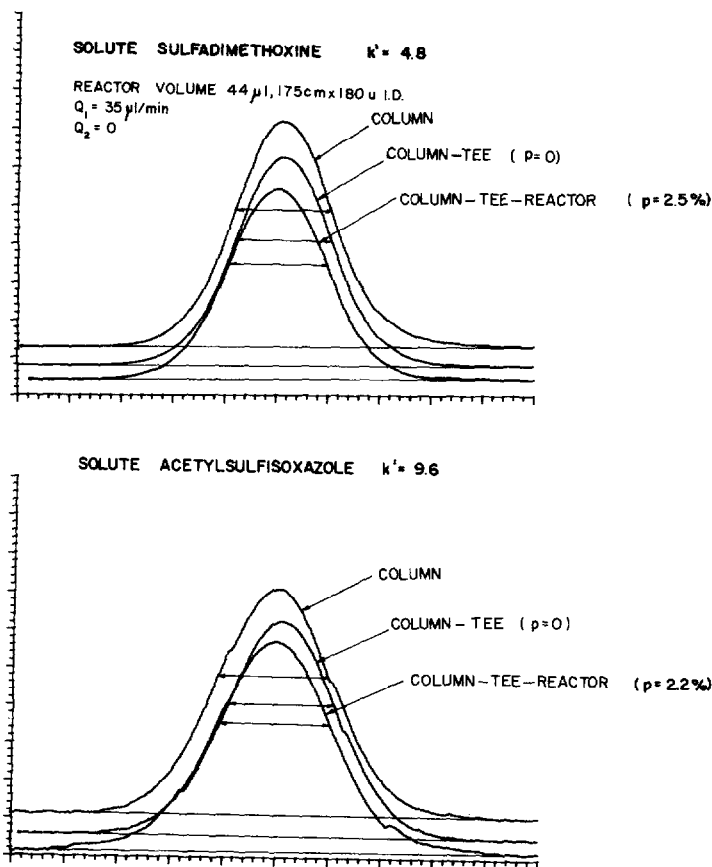


Fig. 7. Band spreading of sulfa drugs in post-column derivatization system.

enon, as described by various workers^{18,19}, and to improve the mixing. A similar experiment was carried out to examine the band spreading obtained from reactors of different volumes. All conditions remaining the same, a stainless-steel 0.009 in. I.D. tubing, 300 cm initial length, was used as the reactor. The reactor volume was varied by sequentially cutting off a 50-cm length after each experiment was completed.

The effect of the secondary flow through the reactor on the band spreading of OPA-amino acid adducts was studied at a constant flow-rate of the mobile phase through the column of $22 \mu\text{l}/\text{min}$. A mixture containing five amino acids was chromatographed and post-column derivatized using a short, $10 \text{cm} \times 0.01 \text{in. I.D.}$, stainless-steel reactor with the OPA reagent flow varied from 7 to $80 \mu\text{l}/\text{min}$. Results obtained from these experiments are shown in Figs. 8 and 9 as plots of the second statistical moment or the volume variance against the reactor volume, square of the reactor diameter, and the square of the flow-rate parameter (ψ), respectively, for adducts corresponding to solutes of different capacity factors. It can be seen that, even with the zig-zagged reactor employed, linearity of the variance with D_r^2 and V_r is well established, which indicates that the Taylor equation²⁰ for the unretained solute can be modified in this case by a simple constant. Intercepts of the graphs shown in

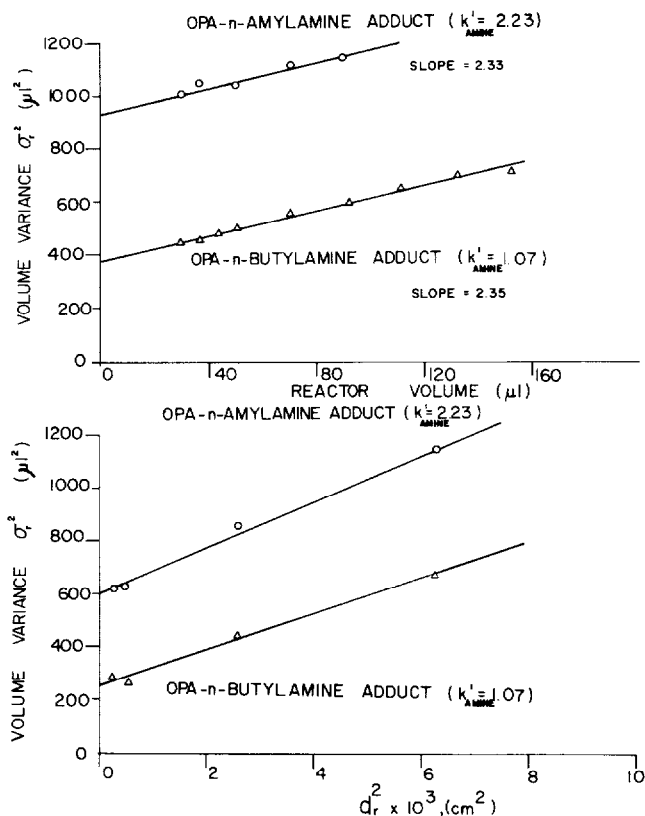


Fig. 8. Graphs of volume variance against reactor volume and the square of reactor diameter for two retained solutes.

Fig. 8 vary because of the fact that two different ODS microbore columns were employed in these experiments. The diffusion coefficients of the OPA adducts used were calculated from the Wilke–Chang equation²¹ and were found to be 0.2×10^{-5} cm^2/sec for both. It was found that the total variance estimated from eqn. 5 was about two times larger than the variance experimentally determined from the slope of σ_v^2/V_R curves, which means that a significant improvement in the reactor performance can be achieved by changing the flow pattern of the moving liquid stream. This has been discussed by various workers^{22,23}. Fig. 9 shows the plot of volume variance vs. the square of the flow-rate parameter, ψ , and it can be seen that σ_v^2 increases linearly with ψ^2 . Since peak height decreases with the factor ψ , a relatively small secondary flow of reagent corresponding to $\psi \approx 1.5$ –2 should be selected in order to minimize the band spreading in the reactor and to ensure that a sufficient amount of reagent is used for the given reaction.

Applications of post-column reaction system

A mixture of homologous *n*-alkylamines starting from methylamine to hexylamine was used to evaluate the designed apparatus. Under the adverse conditions of a relatively large reactor, 175 cm \times 180 μm I.D., and 44 μl volume, the alkylamines

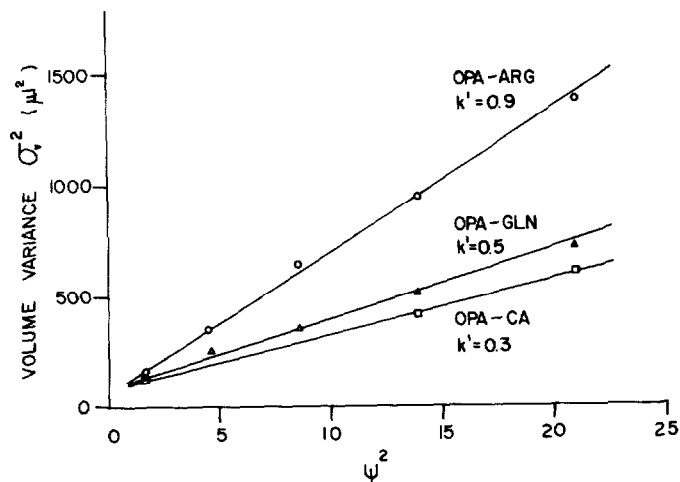


Fig. 9. Graphs demonstrating the dependence of band spreading on the square of the column flow parameter, ψ , for solutes of different k' .

were separated on an Alltech 50 cm \times 1 mm I.D. column packed with Zorbax ODS 7- μ m particles and were derivatized as they emerged from the column with OPA-3-mercaptopropionic reagent. An identical flow-rate of 35 μ l/min for the column and reagent was employed and the mobile phase used was 38% (v/v) acetonitrile in 0.01 M KH_2PO_4 buffer, pH 3.0. A total mass of 40 pmole of each amine was injected onto the column using a 0.2 μ l sample volume. The results obtained are shown in Fig. 10. The top chromatogram was obtained with a conventional 5- μ l fluorescence detector cell, and the bottom chromatogram was recorded with a specially designed 0.25- μ l

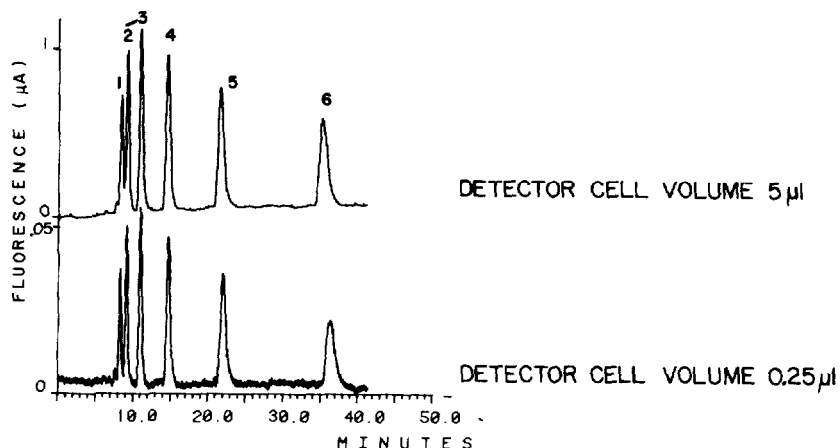


Fig. 10. Chromatograms illustrating differences in sensitivity and resolution resulting from the use of different detector cell volumes. Conditions: column, Alltech ODS 7 μ m particles, 50 cm \times 1 mm; flow-rate, $Q_1 = Q_2 = 35$ μ l/min; mobile phase, 38% acetonitrile in 0.01 M KH_2PO_4 , pH = 3; concentration, 2×10^{-7} mol/ml each solute; injection volume, 0.2 μ l; reactor, 175 cm \times 180 μ m I.D., stainless-steel tubing; derivatization reagent, OPA and 3-mercaptopropionic acid. Solutes: *n*-alkylamines starting from methylamine (1) to hexylamine (6). Top chromatogram was obtained using a 5- μ l detector cell volume, bottom chromatogram with a 0.25- μ l detector cell volume.

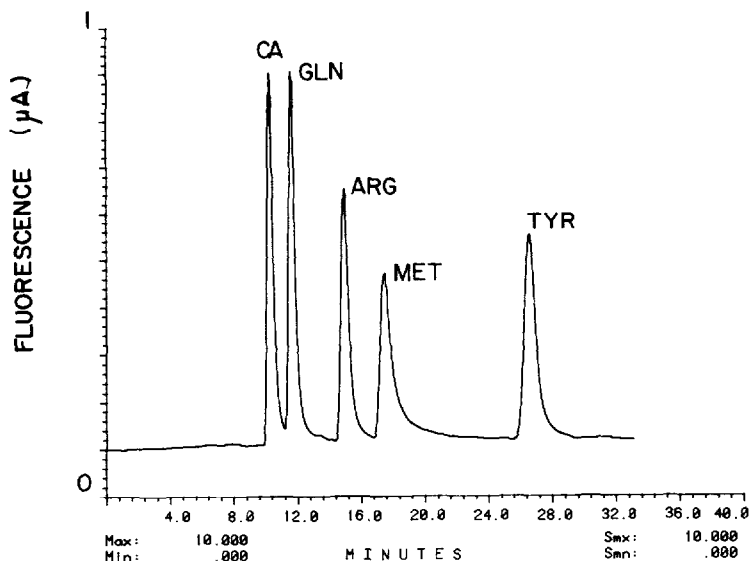


Fig. 11. Analysis of amino acids using a 6-sec post-column derivatization reaction time. Conditions: column, Alltech ODS 7 μm particles, 50 cm \times 1 mm I.D.; flow-rate, $Q_1 = Q_2 = 35 \mu\text{l}/\text{min}$; mobile phase, 0.003 M KH_2PO_4 , pH 3-acetonitrile-tetrahydrofuran (98:2:0.2); concentration, 2×10^{-7} mol/ml each test solute; injection volume, 0.2 μl ; reactor volume, 6 μl . Solutes in the order of increasing k' ; CA = cysteic acid, GLN = glutamine, ARG = arginine, MET = methionine, TYR = tyrosine. Detector cell volume 5 μl .

cell²⁴. It can be seen that, with all other conditions remaining the same, an improvement in the resolution of alkylamines is clearly demonstrated when the special low-volume fluorescence cell is used. However, the reduction of the detector cell volume from 5 to 0.25 μl decreases the number of molecules in the cell that can fluoresce by a factor of 20 and, although the noise remained unchanged, a loss of detector sensitivity by a factor of 20 was observed.

The detection limit of primary amines, using a 5- μl fluorescence cell corresponding to two times the signal-to-noise ratio, was 500 fmoles. In most instances, the volume of peaks eluted from microbore columns are between 15 and 100 μl ; thus, a detector cell volume of 1 μl can be tolerated.

Separation of primary amino acids under operating conditions similar to those used in the previous chromatogram may be seen in Fig. 11. In this case, however, no reactor coil was employed and the low-volume mixing chamber was connected directly to the 5- μl conventional fluorescence cell through a 10 cm \times 0.01 in. I.D. stainless-steel tubing permanently attached to the detector cell. At a combined column and reagent flow equal to 1.2 $\mu\text{l}/\text{sec}$ through the detector connecting tubing 6 μl in volume, which was employed as the reactor in this case, there still was sufficient time for the solute to reach maximum fluorescence because of the very fast reaction employed. Considering the simplicity of this experimental arrangement, and the excellent detection limit of 200 fmoles obtained for these amino acids, the use of the instrumentation and derivatization reaction may have great importance in the analysis of proteins and amino acids.

CONCLUSIONS

The decrease in sensitivity of the microbore system due to the reduction in column diameter has been a subject of much discussion in the past. As the chromatographic column is scaled down, the peak volume and, accordingly, the detector cell volume have to be reduced by a factor corresponding to the square of the ratio of the respective column diameters¹, which could reduce the sensitivity of detection. However, recently designed microbore cylindrical detector cells of longer pathlength and the newly available high-sensitivity detectors allow operation of microbore columns nowadays at the same response-to-noise ratio as the 4.6 mm I.D. columns*.

The results of this study show that the sensitivity of the detection may be increased further with a simple post-column derivatization technique based on the fast OPA reaction with primary amines, modified to include 3-mercaptopropionic acid reagent in order to achieve solute detectability at the level of 10^{-15} mole. As demonstrated previously, one advantage of microcolumns is clearly apparent—the system is ideally suited to microanalysis where a limited amount of sample is available, and to cases where economy of the mobile and the stationary phase is important. While there is a general understanding that a chromatographic system utilizing packed columns is inherently better suited to analytical work in liquid chromatography than a system based on the open-tubular capillary columns, the reverse is true for a reactor for post-column derivatization. Due to the rapid drop of theoretical plates with k' , the best performance of open-tubular capillaries is achieved for an unretained solute. Considering that the diameter of the capillary reactor equals the particle diameter of the packed reactor ($D_c = 1$ mm), much better performance and about 30 times less pressure will be obtained for the capillary reactor. Thus, assuming that nearly ideal mixing is achieved for the sample components entering the reactor, the use of a long, open-tubular, capillary zig-zagged reactor with a narrow diameter, which will assure a high number of theoretical plates, is preferable. Also, the utilization of fast reactions for post-microbore column derivatization is advantageous since slow reaction kinetics would require a segmented flow reactor design in order to keep the band spreading at an acceptable value.

APPENDIX

The chromatographic elution curve, $C = f(t)$, as a typical distribution curve can be characterized by the so-called statistical moments²⁵⁻²⁸

$$M_k = \frac{\int_0^{\infty} f(t) \cdot t^k \, dt}{\int_0^{\infty} f(t) \cdot dt} \quad (1a)$$

where M_k is the k th ordinary statistical moment and $f(t)$ is the solute concentration at the time t . The variance, m_2 , or the second statistical moment about the mean can be defined as

* 1- μ l Fluorescence detectors for use with microbore columns are currently available from Farrand Optical Company, Valhalla, NY, U.S.A. and Ikatos Analytical Instruments, Ramsey, NJ, U.S.A.

$$m_2 = \frac{\int_0^{\infty} f(t) [t - M_1]^2 dt}{\int_0^{\infty} f(t) dt} \quad (2a)$$

In order to simplify the calculations and to make them amenable to computer systems operated on the digital data, the previous equation was simplified as follows:

$$m_2 = \frac{\int_0^{\infty} f(t)t^2 dt - 2 \cdot \int_0^{\infty} f(t) \cdot M_1 t dt + M_1^2 \cdot \int_0^{\infty} f(t) dt}{\int_0^{\infty} f(t) dt} =$$

$$\frac{\int_0^{\infty} f(t)t^2 dt}{\int_0^{\infty} f(t) dt} - \left[\frac{\int_0^{\infty} f(t) \cdot t dt}{\int_0^{\infty} f(t) dt} \right]^2 = M_2 - M_1^2 \quad (3a)$$

Similarly, the third statistical moment reflecting the skewness, S , of the elution curve can be calculated as

$$m_3 = M_3 - 3M_1M_2 + 2M_1^3$$

and

$$S = \frac{m_3}{\sigma^3}$$

Assuming that a sufficient number of points, t_i and $f(t_i)$, corresponding to the height of the chromatographic response are collected, the integral in eqn. 2a can be approximated by the sum of its infinitesimal elements. Thus,

$$M_k = \frac{\sum_{i=1}^n H_i t_i^k}{\sum_{i=1}^n H_i} \quad (4a)$$

and

$$m_2 = \left[\frac{\sum_{i=1}^n H_i \cdot t_i^2}{\sum_{i=1}^n H_i} - \left(\frac{\sum_{i=1}^n H_i \cdot t_i}{\sum_{i=1}^n H_i} \right)^2 \right] \quad (5a)$$

Eqn. 5a was used to calculate variance of peaks entering the detector. The CIS computer data system employed can collect up to 15 points per second, which allows a good estimate of the variance. It has been pointed out previously^{29,30} that all estimates of variance or column efficiency, $N = t^2/\sigma^2$, for asymmetric peaks should only be made by moment calculation since a significant error can arise when the tangent method or the inflection point method is employed.

REFERENCES

- 1 P. Kucera, *J. Chromatogr.*, 198 (1980) 93.
- 2 P. Kucera and G. Manius, *J. Chromatogr.*, 216 (1981) 9.
- 3 P. Kucera and G. Manius, *J. Chromatogr.*, 219 (1981) 1.
- 4 P. Kucera, S. A. Moros and A. R. Mlodozeniec, *J. Chromatogr.*, 210 (1981) 373.
- 5 R. P. W. Scott and P. Kucera, *J. Chromatogr.*, 169 (1979) 51.
- 6 R. P. W. Scott and P. Kucera, *J. Chromatogr.*, 185 (1979) 27.
- 7 J. T. Steward, *Trends Anal. Chem.*, 1 (1982) 170.
- 8 J. F. K. Huber, K. M. Jonker and H. Poppe, *Anal. Chem.*, 52 (1980) 2.
- 9 H. Poppe, *Anal. Chim. Acta*, 114 (1980) 59.
- 10 J. F. K. Huber, *J. Chromatogr. Sci.*, 7 (1969) 172.
- 11 R. P. W. Scott and P. Kucera, *J. Chromatogr. Sci.*, 9 (1971) 641.
- 12 S. S. Simons and D. J. Johnson, *J. Amer. Chem. Soc.*, 98 (1976) 7098.
- 13 S. S. Simons and D. J. Johnson, *Anal. Biochem.*, 82 (1977) 250.
- 14 H. Umagat, P. Kucera and L.-F. Wen, *J. Chromatogr.*, 239 (1982) 463.
- 15 S. D. Stearns, Valco Instruments, Houston, TX, personal communication.
- 16 J. M. Reijn, W. E. van der Linden and H. Poppe, *Anal. Chim. Acta*, 114 (1980) 105.
- 17 R. S. Deelder, A. T. J. M. Kuijpers and J. H. M. van den Berg, *J. Chromatogr.*, 255 (1983) 545.
- 18 R. S. Deelder, M. G. F. Kroll, A. J. B. Beeren and J. H. M. van den Berg, *J. Chromatogr.*, 149 (1978) 669.
- 19 R. Tijssen, *Thesis*, Technical University of Delft, Delft, 1979.
- 20 G. Taylor, *Proc. R. Soc. London, Ser. A*, 219 (1953) 186.
- 21 Wilkes and Chang, *AIChE J.*, 1 (1955) 264.
- 22 I. Halász, *J. Chromatogr.*, 173 (1979) 229.
- 23 K. Hofmann and I. Halász, *J. Chromatogr.*, 199 (1980) 3.
- 24 D. M. Schoeffel and A. K. Sonnenschein, *U.S. Pat.*, 4,088,407, 1978.
- 25 O. Grubner, *Anal. Chem.*, 43 (1971) 1934.
- 26 E. Kučera, *J. Chromatogr.*, 19 (1965) 237.
- 27 O. Grubner, *Advan. Chromatogr.*, 6 (1968) 173.
- 28 E. Grushka, *J. Phys. Chem.*, (1972) 2586.
- 29 J. Higgins, *Computerized Column Testing by the Statistical Moments Method*, Technical Note No. 912, Brownlee Labs., 1979.
- 30 M. C. Harvey, S. D. Stearns and J. W. Nelson, *Determining HPLC Variance with the SP4100 Computing Integrator*, Technical Note, Valco Instruments, Houston, TX.